

## Electronic Supplementary Information (ESI)

### **Tuning the fluorescence sensing for Fe<sup>3+</sup> ions by using different dipyridyl linkers in pillar-layered metal-organic frameworks**

Yan-E Liu‡, Ye Zhou‡, Xiao-Yu Li, Yao Jun, Qiu-Xia Li, Quan-Qing Xu, Rong-Rong Zhu\* and Ai-Xin Zhu\*

Faculty of Chemistry and Chemical Engineering, Yunnan Normal University, Kunming 650500, China.

‡ These authors contributed equally to this paper.

\* Corresponding author.

E-mail: chemzrr1993@163.com (Rong-Rong Zhu); zaxchem@126.com (Ai-Xin Zhu)

Tel: +86 0871 65941088

## Table of Contents

<b>Fig. S1</b> PXRD patterns of <b>PL-1</b> , <b>PL-2</b> , and <b>PL-3</b> .....	<b>1</b>
<b>Fig. S2</b> Solid-state excitation and emission spectra of ligands and MOFs.....	<b>1</b>
<b>Fig. S3</b> The comparison of the luminescence intensities of <b>PL-1</b> , <b>PL-2</b> , and <b>PL-3</b> dispersed in EtOH upon the addition of 400 $\mu$ L of various anions of $\text{Fe}^{3+}$ solutions (10 mM) .....	<b>2</b>
<b>Fig. S4</b> PXRD patterns of <b>PL-1</b> , <b>PL-2</b> , and <b>PL-3</b> after 5 cycles for sensing $\text{Fe}^{3+}$ ions.....	<b>2</b>
<b>Fig. S5</b> PXRD patterns of <b>PL-1</b> , <b>PL-2</b> , and <b>PL-3</b> after being soaked in different metal solutions .....	<b>3</b>
<b>Fig. S6</b> Photographs of <b>PL-1</b> , <b>PL-2</b> , <b>PL-3</b> and $\text{Fe}^{3+}$ incorporated <b>PL-1</b> , <b>PL-2</b> , <b>PL-3</b> .....	<b>3</b>
<b>Fig. S7</b> XPS survey and O1s XPS spectra of <b>PL-1</b> , <b>PL-2</b> , and <b>PL-3</b> before and after being immersed in EtOH solutions of $\text{Fe}(\text{NO}_3)_3$ .....	<b>3</b>
<b>Fig. S8</b> S2p and N1s XPS spectra of <b>PL-1</b> , <b>PL-2</b> , and <b>PL-3</b> before and after being immersed in EtOH solutions of $\text{Fe}(\text{NO}_3)_3$ .....	<b>4</b>
<b>Fig. S9</b> Excitation spectra of <b>PL-1</b> , <b>PL-2</b> , and <b>PL-3</b> dispersed in EtOH and UV-vis absorption spectrum of $\text{Fe}^{3+}$ ions in EtOH .....	<b>4</b>
<b>Fig. S10</b> Polts of adsorption capacities of $\text{Fe}^{3+}$ ions vs. the adsorption time for <b>PL-1</b> , <b>PL-2</b> , and <b>PL-3</b> .....	<b>5</b>
<b>Fig. S11</b> Lengths of pillar for <b>PL-1</b> , <b>PL-2</b> , and <b>PL-3</b> .....	<b>5</b>
<b>Table S1</b> Summary of the values of $K_{\text{SV}}$ for the fluorescent MOFs used for sensing $\text{Fe}^{3+}$ ions .....	<b>6</b>
<b>Table S2</b> List of the structure parameters and $K_{\text{SV}}$ for the pillar-layered MOFs .....	<b>7</b>
<b>References</b> .....	<b>7</b>

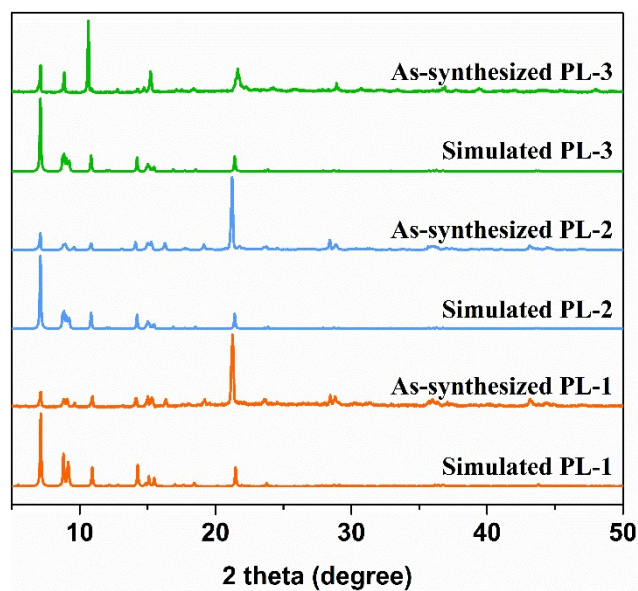


Fig. S1 PXRD patterns of PL-1, PL-2, and PL-3.

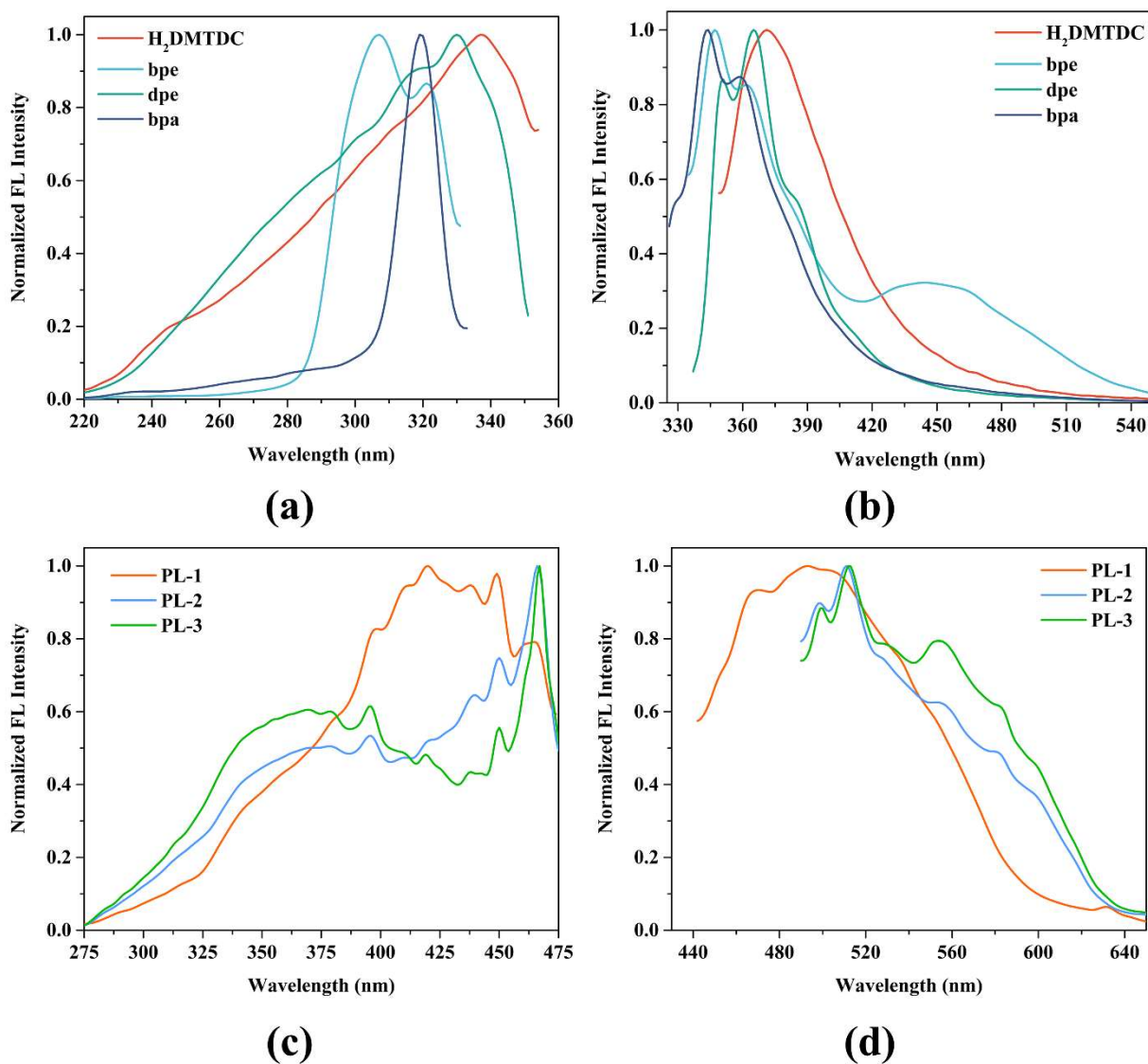
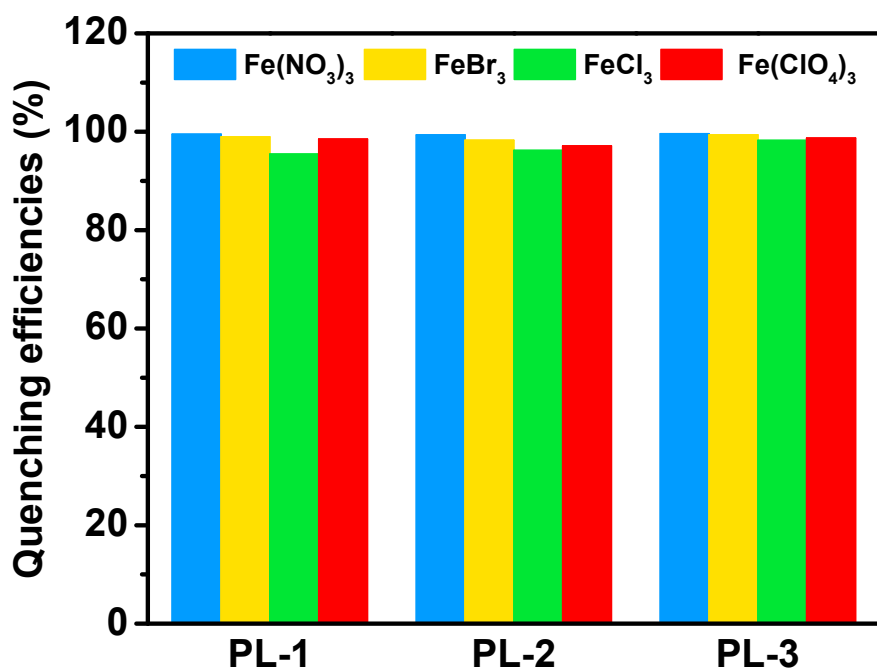
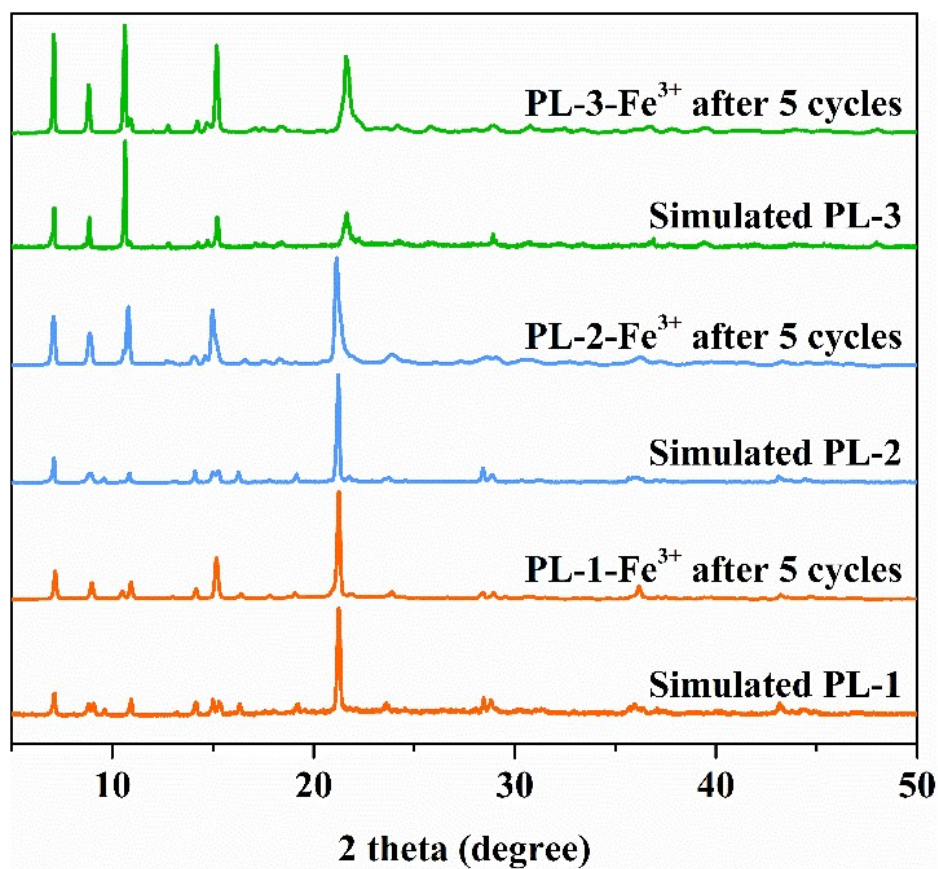


Fig. S2 Solid-state excitation (a, c) and emission (b, d) spectra of ligands and MOFs.



**Fig. S3** The comparison of the quenching efficiency of PL-1, PL-2, and PL-3 dispersed in EtOH upon the addition of 400 μL of various anions of Fe<sup>3+</sup> solutions (10 mM).



**Fig. S4** PXRD patterns of PL-1, PL-2, and PL-3 after 5 cycles for sensing Fe<sup>3+</sup> ions.

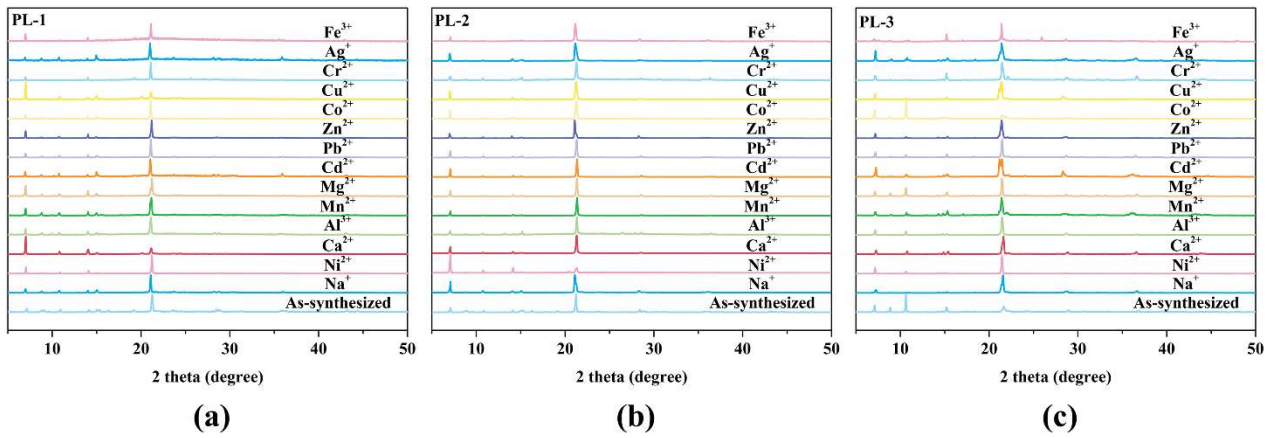


Fig. S5 PXRD patterns of PL-1 (a), PL-2 (b), and PL-3 (c) after being soaked in different metal solutions.

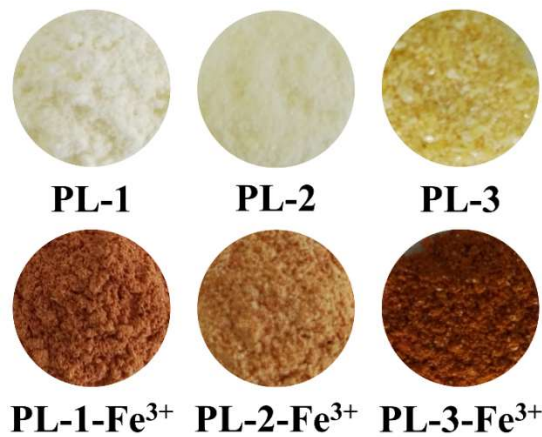


Fig. S6 Photographs of PL-1, PL-2, PL-3 and Fe<sup>3+</sup> incorporated PL-1, PL-2, PL-3.

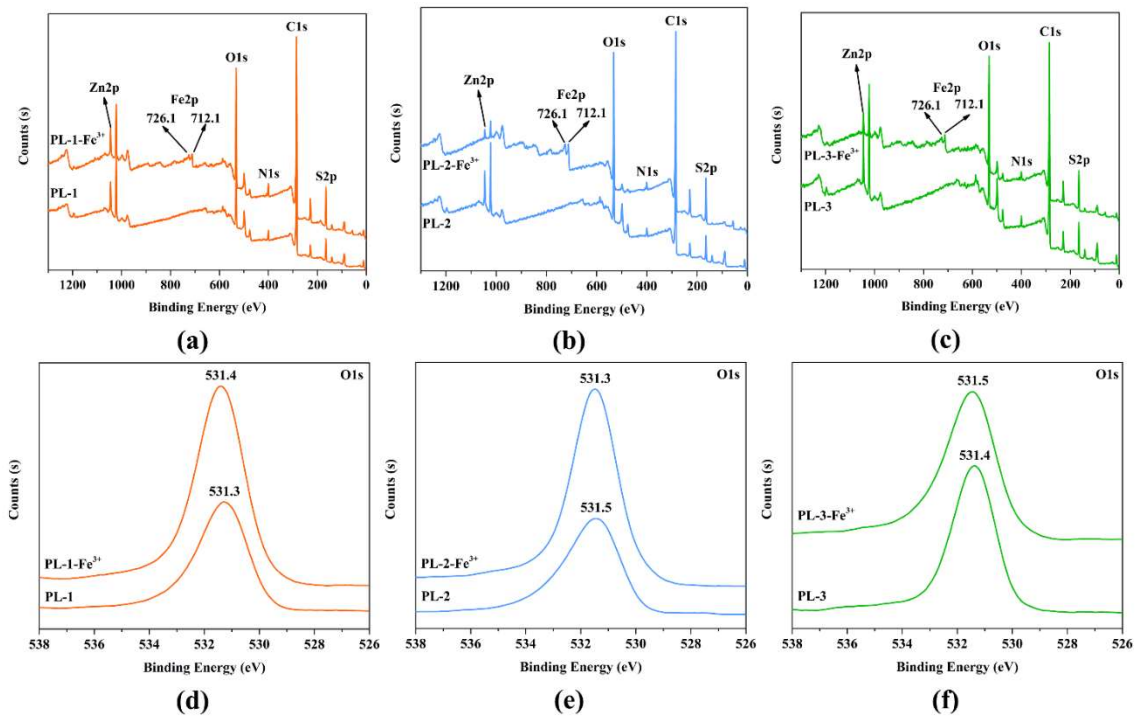
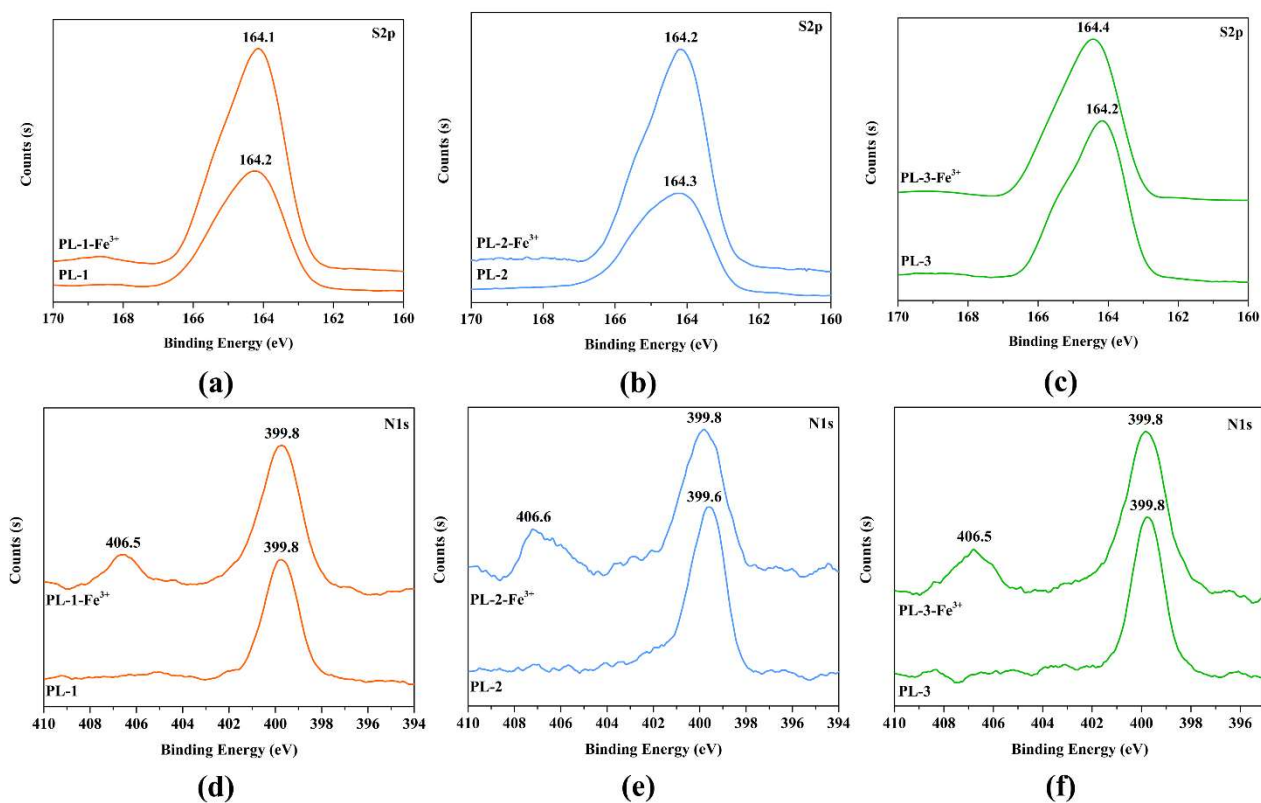
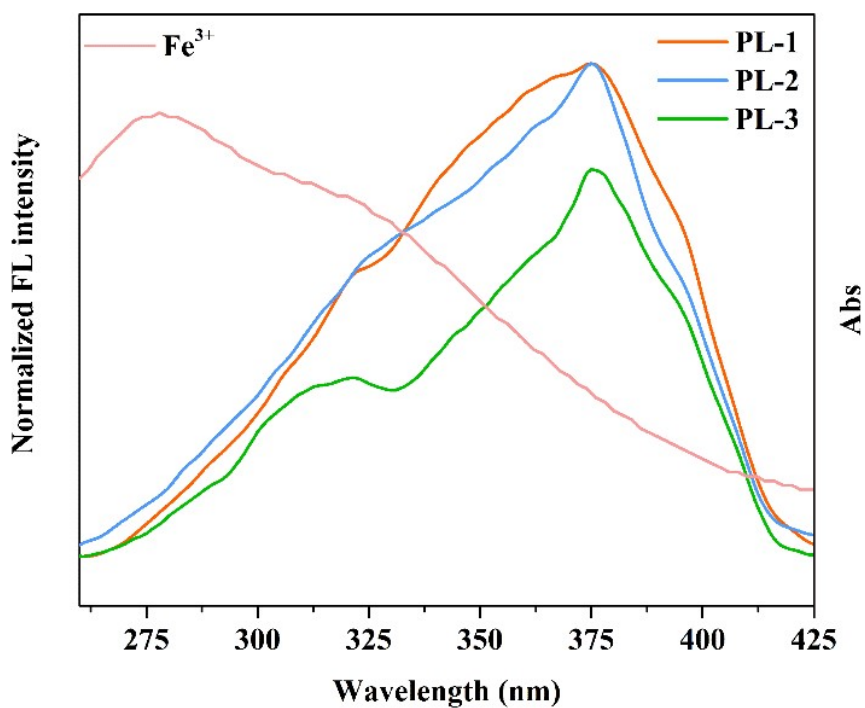


Fig. S7 XPS survey (a, b, c) and O1s XPS spectra (d, e, f) of PL-1, PL-2, and PL-3 before and after being immersed in EtOH solutions of Fe(NO<sub>3</sub>)<sub>3</sub>.



**Fig. S8** S2p (a, b, c) and N1s (d, e, f) XPS spectra of **PL-1**, **PL-2**, and **PL-3** before and after being immersed in EtOH solutions of Fe(NO<sub>3</sub>)<sub>3</sub>.



**Fig. S9** Excitation spectra of **PL-1**, **PL-2**, and **PL-3** dispersed in EtOH and UV-vis absorption spectrum of Fe<sup>3+</sup> ions in EtOH.

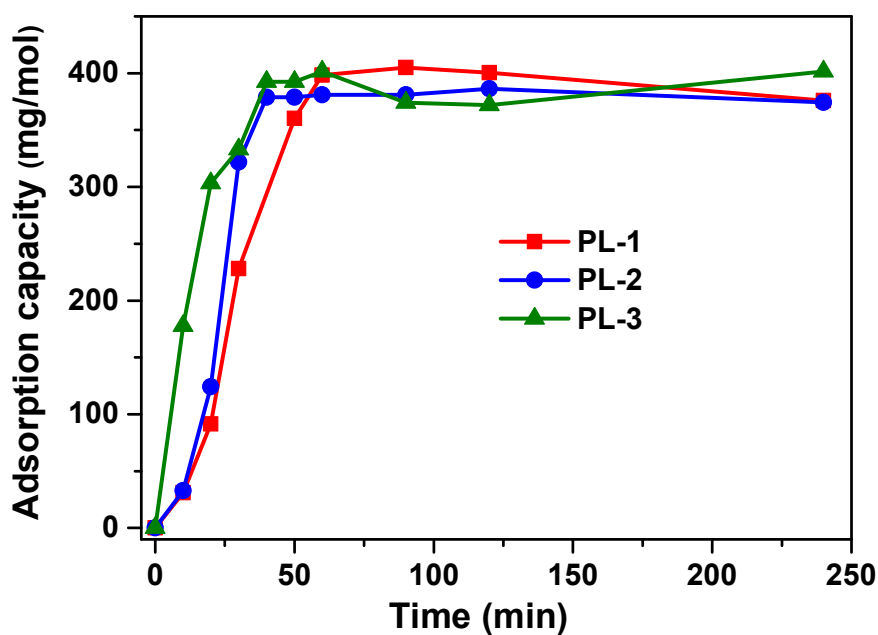


**Fig. S10** Plots of adsorption capacities of  $\text{Fe}^{3+}$  ions vs. the adsorption time for **PL-1**, **PL-2**, and **PL-3**. The saturated adsorption capacity for  $\text{Fe}^{3+}$  ions is comparable for **PL-1**, **PL-2** and **PL-3** with *ca.* 376, 374, and 402 mg/mol at 4 h, respectively. The adsorption rate (from the slope for this curve) below 30 min obviously follows the order: **PL-3** > **PL-2** > **PL-1**.

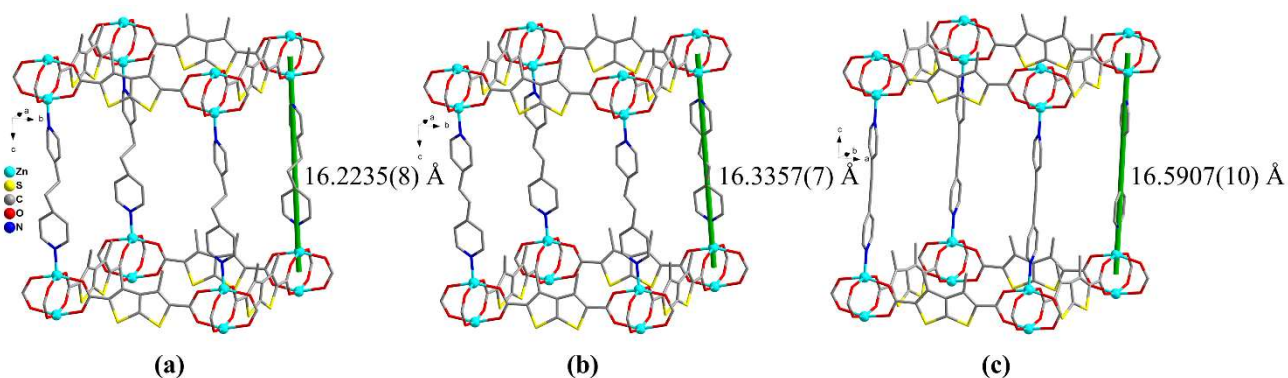


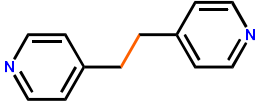
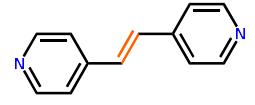
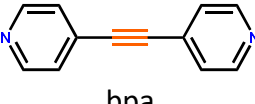
**Fig. S11** Lengths of pillar for **PL-1** (a), **PL-2** (b), and **PL-3** (c).

**Table S1** Summary of the values of  $K_{SV}$  for the fluorescent MOFs used for sensing  $Fe^{3+}$  ions.

Fluorescent MOF materials	Media	$K_{SV}$ ( $M^{-1}$ )	Ref.
$\{[Cd_2(bptc)(2,2'-bipy)_2(H_2O)_2]\}_n$	H <sub>2</sub> O	$8.61 \times 10^3$	S1
$\{[Cd_2(bptc)(phen)_2] \cdot 4H_2O\}_n$	H <sub>2</sub> O	$3.07 \times 10^3$	S1
$\{[Cd_2(bptc)(4,4'-bipy)(H_2O)_2] \cdot 4H_2O\}_n$	H <sub>2</sub> O	$6.21 \times 10^3$	S1
$[Zn_2(trz)_2(btdb)] \cdot 4DMF$	H <sub>2</sub> O	$2.4 \times 10^2$	S2
$[Cd_{1.5}(L)_2(bpy)(NO_3)]$	H <sub>2</sub> O	$1.13 \times 10^4$	S3
$[Eu(BCB)(DMF)] \cdot (DMF)_{1.5}(H_2O)_2$	H <sub>2</sub> O	$2.35 \times 10^4$	S4
$[Zn(DHT)(BPP)]_n$	H <sub>2</sub> O	$1.77 \times 10^4$	S5
$[Cd_{1.5}(L)_2(bpy)(NO_3)]$	H <sub>2</sub> O	$1.91 \times 10^4$	S6
$[Eu_2(L)_3(DMF)_2(H_2O)_4] \cdot 2DMF$	H <sub>2</sub> O	$8.31 \times 10^3$	S7
$[Tb_2(L)_3(DMF)_2(H_2O)_4] \cdot 2DMF$	H <sub>2</sub> O	$5.63 \times 10^3$	S7
$[Gd_2(L)_3(DMF)_2(H_2O)_4] \cdot 2DMF$	H <sub>2</sub> O	$2.86 \times 10^4$	S7
$[Y_2(L)_3(DMF)_2(H_2O)_4] \cdot 2DMF$	H <sub>2</sub> O	$1.50 \times 10^4$	S7
$[Co_6(oba)_4(Hatz)(atz)(H_2O)_2(\mu_3-OH)_2(\mu_2-OH)] \cdot H_2O$	H <sub>2</sub> O	$9.61 \times 10^4$	S8
UiO-67	H <sub>2</sub> O	$5.981 \times 10^4$	S9
UiO-67@N	H <sub>2</sub> O	$5.252 \times 10^4$	S9
UiO-67@NN	H <sub>2</sub> O	$1.646 \times 10^4$	S9
$\{[Zn_4(tpta)_2(OH)_2(bib)_4] \cdot H_2O\}_n$	H <sub>2</sub> O	$7.8 \times 10^3$	S10
JLUMOF201-Y	H <sub>2</sub> O	$7.67 \times 10^3$	S11
JLUMOF201-Tb	H <sub>2</sub> O	$8.38 \times 10^3$	S11
$\{[H_2N(Me)_2]_2[Zn_5(L)_2(OH)_2] \cdot 3DMF \cdot 4H_2O\}_n$	H <sub>2</sub> O	$9.799 \times 10^4$	S12
$[Zn_2(trz)_2(btdb)] \cdot 4DMF$	MeOH	$3.3 \times 10^3$	S2
$[Eu_2(TDC)_3(CH_3OH)_2(CH_3OH)]$	MeOH	$3.42 \times 10^3$	S13
$[Tb_2(TDC)_3(CH_3OH)_2(CH_3OH)]$	MeOH	$3.04 \times 10^4$	S13
$[Cd_2(L1)(tdc)_2(H_2O)]_n$	EtOH	$3.01 \times 10^3$	S14
$[Cd(L2)_{0.5}(tdc)]_n$	EtOH	$4.22 \times 10^3$	S14
Tb <sup>3+</sup> @Zn-MOF	EtOH	$3.26 \times 10^4$	S15
$CH_3-dpb)_2[Mg_3(1,4-NDC)_4(\mu-H_2O)_2(CH_3OH)(H_2O)] \cdot 1.5H_2O$	EtOH	$1.6 \times 10^4$	S16
$[La(TPT)(DMSO)_2] \cdot H_2O$	EtOH	$1.36 \times 10^4$	S17
EuL <sub>3</sub>	EtOH	$4.1 \times 10^3$	S18
$[Eu_2K_2(dcpa)_2(H_2O)_6] \cdot 5H_2O$	EtOH	$4.30 \times 10^4$	S19
$[Eu_3(FDA)_4(DMSO)_2(NO_3)(H_2O)_2]_n$	EtOH	$3.3 \times 10^4$	S20
PL-1	EtOH	$1.58 \times 10^4$	This work
PL-2	EtOH	$1.72 \times 10^4$	This work
PL-3	EtOH	$2.47 \times 10^4$	This work



**Table S2** List of the structure parameters and  $K_{SV}$  for the pillar-layered MOFs.

MOFs	Dipyridyl ligand	Length of the pillar (Å)	Pore volume (%)	$K_{SV}$ (M <sup>-1</sup> )
PL-1	 bpe	16.2235(8)	45.5	1.60 x 10 <sup>4</sup>
PL-2	 dpe	16.3357(7)	45.7	1.73 x 10 <sup>4</sup>
PL-3	 bpa	16.5907(10)	46.0	2.52 x 10 <sup>4</sup>

## References

- S1. Y. Lin, X. Zhang, W. Chen, W. Shi and P. Cheng, *Inorg. Chem.*, 2017, **56**, 11768-11778.
- S2. X.-T. Hu, Z. Yin, X.-P. Luo, C.-H. Shen and M.-H. Zeng, *Inorg. Chem. Commun.*, 2021, **129**, 108664.
- S3. M. Singh, S. Senthilkumar, S. Rajput and S. Neogi, *Inorg. Chem.*, 2020, **59**, 3012-3025.
- S4. M. Y. Zhang, F. Y. Yi, L. J. Liu, G. P. Yan, H. Liu and J. F. Guo, *Dalton Trans.*, 2021, **50**, 15593-15601.
- S5. S. T. Wang, X. Zheng, S. H. Zhang, G. Z. Li and Y. Xiao, *CrystEngComm*, 2021, **23**, 4059-4068.
- S6. M. Singh, G. Kumar and S. Neogi, *Front. Chem.*, 2021, **9**, 651866.
- S7. L. J. Zhao, B. Li and G. P. Yong, *CrystEngComm*, 2023, **25**, 2813-2823.
- S8. W. S. Zhang, G. Q. Wang, Y. X. Wang, Y. L. Yang, X. Bai, H. Cui, Y. Lu and S. X. Liu, *Dalton Trans.*, 2023, **52**, 4407-4414.
- S9. S. Fajal, W. Mandal, D. Majumder, M. M. Shirolkar, Y. D. More and S. K. Ghosh, *Chem. Eur. J.*, 2022, **28**, e202104175.
- S10. D. Qi, X. Si, L. Guo, Z. Yan, C. Shao and L. Yang, *Colloid and Surfaces A*, 2022, **649**, 129477.
- S11. Q. Hu, T. Xu, J. Gu, L. Zhang and Y. Liu, *CrystEngComm*, 2022, **24**, 2759-2766.
- S12. Y.-T. Yan, Y.-L. Wu, L.-N. Zheng, W. Cai, P.-F. Tang, W.-P. Wu, W.-Y. Zhang and Y.-Y. Wang, *New J. Chem.*,

- 2022, **46**, 4292–4299.
- S13. K. Xu, F. Wang, S. Huang, Z. Yu, J. Zhang, J. Yu, H. Gao, Y. Fu, X Li, Y. Zhao, *RSC Adv.*, 2016, **6**, 91741-91747.
- S14. Y. Q. Su, L. Fu and G. H. Cui, *Dalton Trans.*, 2021, **50**, 15743-15753.
- S15. Y.-J. Liang, J. Yao, M. Deng, Y.-E. Liu, Q.-Q. Xu, Q.-X. Li, B. Jing, A.-X. Zhu and B. Huang, *CrystEngComm*, 2021, **23**, 7348-7357.
- S16. Z. F. Wu, L. K. Gong and X. Y. Huang, *Inorg. Chem.*, 2017, **56**, 7397-7403.
- S17. C. Zhang, Y. Yan, Q. Pan, L. Sun, H. He, Y. Liu, Z. Liang J. Li, *Dalton Trans.*, 2015, **44**, 13340 -13346.
- S18. M. Zheng, H. Tan, Z. Xie, L. Zhang, X. Jing Z. Sun, *ACS Appl. Mater. Interfaces*. 2013, **5**, 1078-1083.
- S19. H. Zhang, R. Fan, W. Chen, J. Fan, Y. Dong, Y. Song, X. Du, P. Wang, Y. Yang, *Cryst. Growth Des.* 2016, **16**, 5429-5440.
- S20. H. Zhang, G.-Y. Liu, X.-H. Diao, Y. Muhammad, C. Chen, Y.-Y. Gao, H. Wang, C.-S. Qi, W. Li, *J. Solid State Chem.*, 2023, **324**, 124114.